

# ENHANCEMENT OF STABILITY ON AUTONOMOUS WAYPOINT MISSION OF QUADROTOR USING LQR INTEGRATOR CONTROL

OKTAF AGNI DHEWA<sup>1</sup>, TRI KUNTORO PRIYAMBODO<sup>2\*</sup>,  
ARIS NASUHA<sup>1</sup> AND YASIR MOHD MUSTAFAH<sup>3</sup>

<sup>1</sup>*Department of Electronics and Informatics Engineering,  
Yogyakarta State University, Yogyakarta, Indonesia*

<sup>2</sup>*Department of Computer Science and Electronics,  
Universitas Gadjah Mada, Yogyakarta, Indonesia*

<sup>3</sup>*Department of Mechatronics Engineering,  
International Islamic University Malaysia,  
Jalan Gombak, 53100 Kuala Lumpur, Malaysia*

*\*Corresponding author: mastri@ugm.ac.id*

*(Received: 26<sup>th</sup> January 2021; Accepted: 1<sup>st</sup> May 2021; Published on-line: 4<sup>th</sup> January 2022)*

**ABSTRACT:** The ability of the quadrotor in the waypoint trajectory tracking becomes an essential requirement in the completion of various missions nowadays. However, the magnitude of steady-state errors and multiple overshoots due to environmental disturbances leads to motion instability. These conditions make the quadrotor experience a shift and even change direction from the reference path. As a result, to minimize steady-state error and multiple overshoots, this study employs a Linear Quadratic Regulator control method with the addition of an Integrator. Comparisons between LQR without Integrator and LQR with Integrator were performed. They were implemented on a quadrotor controller to track square and zig-zag waypoint patterns. From experimental results, LQR without Integrator produce of 2 meters steady-state error and -1.04 meters undershoot average with an accuracy of 64.84 % for square pattern, along 3.19 meters steady-state error, and -1.12 meters undershoot average with an accuracy of 46.73 % for a zig-zag way. The LQR method with integrator produce of 1.06 meters steady-state error with accuracy 94.96 % without multiple-overshoot for square pattern, the 1.06 meters steady-state error, and -0.18 meters undershoot average with an accuracy of 86.49 % for the zig-zag way. The results show that the LQR control method with Integrator can minimize and improve steady-state error and multiple overshoots in quadrotor flight. The condition makes the quadrotor able to flying path waypoints with the correct system specification.

**ABSTRAK:** Kemampuan quadrotor dalam pengesanan lintasan waypoint menjadi syarat penting dalam menyelesaikan pelbagai misi pada masa kini. Walau bagaimanapun, besarnya ralat keadaan mantap dan banyak kelebihan kerana gangguan persekitaran menyebabkan ketidakstabilan pergerakan. Keadaan ini menjadikan quadrotor mengalami pengeseran dan bahkan mengubah arah dari jalur rujukan. Oleh itu, kajian ini menggunakan kaedah kawalan Linear Quadratic Regulator dengan penambahan integrator dalam meminimumkan ralat keadaan mantap dan banyak kelebihan. Perbandingan antara LQR tanpa Integrator dan LQR dengan Integrator dilakukan. Mereka dilaksanakan pada pengawal quadrotor untuk mengesan corak titik jalan persegi dan zig-zag. Dari hasil eksperimen, LQR tanpa Integrator menghasilkan ralat keadaan mantap 2 meter dan -1.04 meter rata-rata undur tembak dengan ketepatan 64.84% untuk corak persegi, sepanjang ralat keadaan tetap 3.19 meter, dan -1.12 meter rata-rata undur

bawah dengan ketepatan 46.73 % untuk cara zig-zag. Kaedah LQR dengan integrator menghasilkan ralat keadaan mantap 1.06 meter dengan ketepatan 94.96% tanpa tembakan berlebihan untuk corak segi empat sama, ralat keadaan mantap 1.06 meter, dan rata-rata undur tembak -0.18 meter dengan ketepatan 86.49% untuk zig-zag cara. Hasilnya menunjukkan bahawa kaedah kawalan LQR dengan Integrator dapat meminimumkan dan memperbaiki ralat keadaan mantap dan banyak overhoot dalam penerbangan quadrotor. Keadaan tersebut menjadikan quadrotor dapat terbang ke titik jalan dengan spesifikasi sistem yang betul.

---

**KEYWORDS:** *optimal control; quadrotor; stability; waypoint*

## 1. INTRODUCTION

Unmanned aerial vehicle (UAV) is an unmanned aircraft with comfortable and efficient use accessibility [1]. UAV has attracted the attention of invention activists in the industrial, civilian, and military fields to use UAVs as a vehicle to help complete various missions that are being developed [2]. Such as aerial surveillance, reconnaissance, aerial photography, transportation of goods, and many others [3].

Completion of these missions is not only required of UAVs to be able to maintain a stable attitude of orientation and altitude but also expected to have the ability to trace the flight path following a predetermined row of earth location coordinates or called waypoints mission. The completeness of the existing capabilities makes UAVs map an area precisely and accurately, which is also the main requirement for developing various current missions [4][5].

Along with advances in technological science, many UAVs have experienced improvements in both physical form patterns and flight systems to achieve specific mission operational targets. One of these UAVs is a quadrotor, which uses four motor actuators as a flight driver. More broadly, a quadrotor is a UAV that can take off and land vertically (VTOL) even in a limited area [6]. A quadrotor also has a constant flight speed to hover in a specific location with its stationary motion [7].

Looking deeply at the quadrotor architecture, the potential capabilities of quadrotors do not necessarily exist by themselves. It was still built through the involvement of several relatively complex system infrastructures. There is one system in all existing quadrotor system infrastructure that plays a vital role as a determining factor in the flight process. The system is a quadrotor flight control system. Without a well-managed control system, the quadrotor cannot maintain rotational or translation movements, causing the plane's crash.

As previously mentioned, quadrotor motion control is divided into two categories: controlling rotational motion and translational motion. The quadrotor motion control started from rotational movement and was followed by translational motion with rules accommodated by a particular control method to achieve a stable state. By referring to several studies conducted by [8] and [9], which focus on controlling quadrotor rotational attitudes, the vehicle can have good flight stability by applying the Linear Quadratic Regulator (LQR) control system method full state feedback. The author's research explains that the LQR method provides regulatory characteristics in the control signal by forcing the control signal to a value close to zero. LQR control makes the system able to overcome errors through a fast response. This statement was strengthened from several other studies, such as applying LQR control methods on UAV aircraft that are more effective and robust

than PID control to a stable system [10]. LQR can maintain system stability in less than 1 second, producing shallow errors [11,12].

However, referring to other research literature regarding the performance of LQR control, it indicates that this method is not good enough to accommodate the translational motion of an object with a significant average deviation that occurs when the system has reached its steady-state [13]. This statement was visualized through research conducted by [14]. The author built an autopilot control system on a quadrotor in moving to the waypoint coordinates using LQR control. In tracing the four waypoint coordinates, the research test found that the quadrotor maintained the anti-rotational motion that met the flight success standards. However, the quadrotor has quite a significant deviation of the mean translational movement of the x and y axes, which is about 2 meters from the reference of the flight path.

The process of tracing the coordinates of the Earth's location on a quadrotor requires a navigation system with data information obtained from the Global Positioning System (GPS) [15]. GPS is a prototype that provides latitude and longitude information at an earth location. Changes in the GPS reading point position converted to the displacement of the x and y axes in meters. The displacement will be used as the error reference value for the quadrotor control to the destination point [16].

The environment disturbance can influence the stability of the quadrotor in the waypoint mission. If the quadrotor has not an eligible control system, it produces more significant error ever. The larger deviation will be accompanied by the results of the steady-state error or the average deviation, which is also getting more significant. This condition causes the quadrotor to experience a shift from the proper track. Also, a steady-state error that diverges with intensity as often as possible will trigger the system to experience multiple overshoots, which result in flight conditions not only shifting but also affecting the aircraft to change direction from the trajectory traced [17].

The main focus of this study is to design by adding the compensation Integrator component to the anatomy structure LQR control method. This compensation involves past information to correct the current signal. This process makes minimize steady-state errors and multiple overshoots in the system. So, the stability of translation motion can be enhanced and managed to track the path correctly.

## 2. QUADROTOR DYNAMICS MODEL

The Newton-Euler equation is necessary to build a quadrotor with flight in x-configuration. This study uses an inertial North-East-Down (NED) frame of reference and a body fixed frame to fulfil this Equation. The NED frame of reference has two axes, N and E, parallel to the north and east and one D axis directed downward towards the center of the Earth, so Newton's first law will apply to this frame of reference. Another frame of reference, the body fixed frame, is indicated by the direction of the x, y, and z axes with a center point that coincides with the center of gravity on the quadrotor body [3]. The two terms of reference are shown in Fig. 1.

In control theory, the dynamic behaviour of a given system can be obtained from its states. There are six quadrotor attitudes related to rotation, namely: Euler angle  $[\phi \ \theta \ \psi]$  (*Roll – Pitch – Yaw*) and angular velocity around each axis body-fixed frame  $[p \ q \ r]$ , for the other six states, namely: from the center of gravity (cog) position  $[x \ y \ z]$  and linear

velocity in  $[x \ y \ z]$ , relative to the body fixed frame. Therefore, the quadrotor has 12 states representing 6 degrees of freedom (DOF) [3].

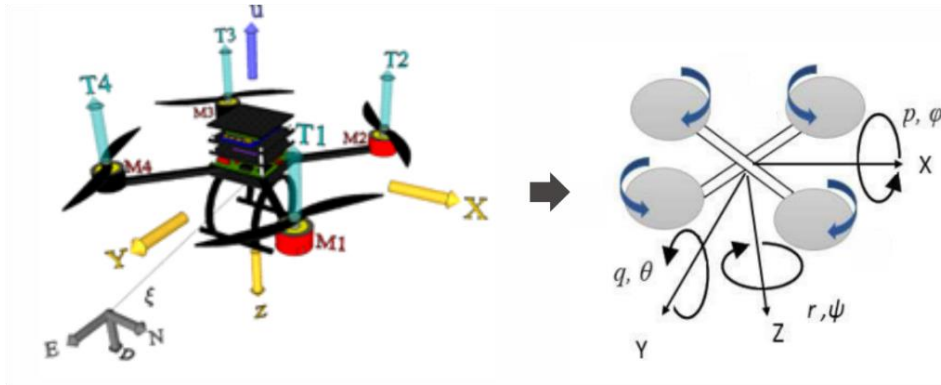


Fig. 1: NED frame of quadrotor.

Quadrotor modelling consists of 3-axis rotational movement (roll, pitch, yaw) and 3-axis translation movement of the Earth's x, y, z-axis (Earth) to the z-axis of the body. Quadrotor translation movement references used in modelling are inertial earth frame (E-frame)  $[E_x \ E_y \ E_z]$  and inertial body frame (B-frame)  $[B_x \ B_y \ B_z]$ .

The rotational movement  $\phi$  (roll) is the quadrotor movement around the y-axis of the body, the rotational movement  $\theta$  (pitch) is the quadrotor movement around the x-axis of the body, and the rotational movement  $\psi$  (yaw) is the quadrotor movement around the z-axis of the body.

The change in the position of the body frame coordinates to the earth frame can be determined by a rotation matrix, where the final position of the body to the earth frame can be determined if the rotation matrix is known, as in Equation (1).

$$\begin{bmatrix} x' \\ y' \\ z' \end{bmatrix} = \begin{bmatrix} x \\ y \\ z \end{bmatrix} \quad (1)$$

Determination of coordinate changes is carried out with a rotational matrix that corresponds to the rotating axis of the body frame. Like when the quadrotor body rotates on the x, y, and z-axis of the body frame, the final position of the coordinates of the body to the earth frame can be found with a rotational matrix which is sequential for each axis through Eq. (2) to Eq. (4)[3].

$$R_x(\phi) = \begin{bmatrix} 1 & 0 & 0 \\ 0 & \cos(\phi) & -\sin(\phi) \\ 0 & \sin(\phi) & \cos(\phi) \end{bmatrix} \quad (2)$$

$$R_y(\theta) = \begin{bmatrix} \cos(\theta) & 0 & \sin(\theta) \\ 0 & 1 & 0 \\ -\sin(\theta) & 0 & \cos(\theta) \end{bmatrix} \quad (3)$$

$$R_z(\psi) = \begin{bmatrix} \cos(\psi) & -\sin(\psi) & 0 \\ \sin(\psi) & \cos(\psi) & 0 \\ 0 & 0 & 1 \end{bmatrix} \quad (4)$$

The three rotational matrix equations create a relationship between body frame coordinates and earth frame coordinates. The relationship is created from the multiplication of the three rotational matrices and is shown in Eq. (5), where c is cos and s is sin.

$$R_B^E(\psi, \theta, \phi) = \begin{bmatrix} c(\psi)c(\theta) & -s(\psi)c(\phi) + c(\psi)s(\theta)s(\phi) & s(\psi)s(\phi) + c(\psi)c(\phi)s(\theta) \\ s(\psi)c(\theta) & c(\psi)s(\theta) + s(\phi)s(\theta)s(\psi) & -c(\psi)s(\phi) + s(\theta)s(\psi)c(\phi) \\ -s(\theta) & c(\theta)s(\phi) & c(\theta)c(\phi) \end{bmatrix} \quad (5)$$

The rotation matrix on the quadrotor used is only the z coordinates of the body frame against the x, y, and z coordinates of the earth frame. The quadrotor can only move up and down along the z coordinates of the body. The movement of the quadrotor at the x and y coordinates of the earth frame is the result of changes in the orientation of the roll angle and pitch from point 00 when the quadrotor moves on the z-axis of the body [3].

Quadrotor modeling is calculated using the Newton-Euler approach, where Newton II's law also applies in the system. Newton's second law describes the relationship between the force  $F$  and the acceleration  $a$  experienced by a center of mass, with the three forces and the acceleration for each axis on the quadrotor, so the relationship is as shown in Eq. (6).

$$F = m \cdot a \quad (6)$$

The quadrotor has a net force determined by the lift force of the four rotors, which can be calculated through Eq. (7).

$$F_T = u_1 = \sum_{i=1}^4 f_i \quad (7)$$

Quadrotor movement on the x, y, and z coordinate axes of the earth frame can be modeled with the rotation matrix of Eq. (5) and Newton II's law in Equation (6). The rotation matrix in the third column of Eq. (5) with the axis used is only the z-axis of the body frame to the x, y, and z axes of the earth frame.

Based on this modeling, the translational motion on the x, y, z axes of the earth frame is described through Eq. (8) and Eq. (10).

$$F_x = F_T \cdot B_{B_x}^{E_z} \quad (8)$$

$$F_y = F_T \cdot B_{B_y}^{E_z} \quad (9)$$

$$F_z = F_T \cdot B_{B_z}^{E_z} + m \cdot g \quad (10)$$

From Eqs. (8) to (10), described by the rotation matrix equation obtained by  $c(\cdot)$  is cos, and  $s(\cdot)$  is sin shown in Eqs. (11) to (13).

$$m \cdot \ddot{x} = F_T (c(\phi)s(\theta)c(\psi) + s(\phi)s(\psi)) \quad (11)$$

$$m \cdot \ddot{y} = F_T (-c(\psi)s(\phi) + s(\theta)s(\psi)c(\phi)) \quad (12)$$

$$m \cdot \ddot{z} = F_T (c(\phi)c(\theta) + m \cdot g) \quad (13)$$

The thrust or  $F_T$  obtained from Eq. (7) will experience a change in pitch angle ( $\theta$ ), roll angle ( $\phi$ ), yaw angle ( $\psi$ ) for translational movement on each axis of the quadrotor earth frame so that Eqs. (11) to (13) can be simplified to,

$$m \cdot \ddot{x} = F_T \cdot s(\theta) \quad (14)$$

$$m \cdot \ddot{y} = F_T (-s(\phi)) \quad (15)$$

$$m \cdot \ddot{z} = F_T + m \cdot g \quad (16)$$

This equation can be further simplified into Eqs. (17) to (19) with a slight angle approximation (close to  $0^\circ$ ) by simulating the value of the angular acceleration  $\sin \alpha$ , and the result is close to the angle  $\alpha$  itself.

$$\ddot{x} = \frac{F_T \cdot \theta}{m} \quad (17)$$

$$\ddot{y} = \frac{F_T \cdot \phi}{m} \quad (18)$$

$$\ddot{z} = \frac{F_T}{m} + g \quad (19)$$

Quadrotor rotational motion modeling can use the second Euler's law. This law describes the relationship between torque ( $\tau$ ) and angular acceleration ( $\alpha$ ) and the relationship between angular momentum ( $L$ ) and rotational speed ( $\omega$ ) for each axis experienced by a center of mass, as shown in Eq. (20).

$$\tau = I \cdot \alpha + L \times \omega \quad (20)$$

with the cross product of momentum and angular velocity, the torque can be solved through Eq. (21),

$$\tau = I \cdot \alpha + L \times \omega \sin \beta \quad (21)$$

$\beta$  is the angle formed by angular momentum and rotational speed. The angle formed in the quadrotor rotation motion is minimal and does not affect so that the angle can be ignored by giving it a zero value. From this, it makes Eq. (21) only affected by the relationship of torque, angular acceleration, and inertia as in Eqs. (22) and (23).

$$\tau = I \cdot \alpha \quad (22)$$

$$\tau = I \cdot \dot{\omega} \quad (23)$$

The relationship  $\tau$  (torque) with lift or (thrust) is shown in Eq. (24).

$$\tau = F \cdot r \quad (24)$$

The matrix component I (inertia) is shown in Eq. (25), and the angular acceleration and angular torque matrix are shown in Eqs. (26) and (27). In contrast, the lift or thrust matrix is shown in Eq. (28).

$$I = \begin{bmatrix} I_{xx} & 0 & 0 \\ 0 & I_{yy} & 0 \\ 0 & 0 & I_{zz} \end{bmatrix} \quad (25)$$

$$\alpha = \begin{bmatrix} \ddot{\phi} \\ \ddot{\theta} \\ \ddot{\psi} \end{bmatrix} \quad (26)$$

$$\tau = \begin{bmatrix} \tau_{\phi} \\ \tau_{\theta} \\ \tau_{\psi} \end{bmatrix} \quad (27)$$

$$F = \begin{bmatrix} F_{\phi} \\ F_{\theta} \\ F_{\psi} \end{bmatrix} \quad (28)$$

The form of roll rotation ( $\phi$ ) and pitch ( $\theta$ ) can be modeled into Eqs. (29) and (30).

$$I_{xx} \cdot \ddot{\phi} = F_{\phi} \cdot r \quad (29)$$

$$I_{yy} \cdot \ddot{\theta} = F_{\theta} \cdot r \quad (30)$$

where,  $I_{xx}$  is the inertia of the quadrotor on the x-axis,  $\ddot{\phi}$  is the angular acceleration of the roll,  $r$  is the distance between the motor and the center of gravity of the quadrotor and  $\tau_{\phi}$  is the roll torque. Also,  $I_{yy}$  is the inertia of the quadrotor on the y-axis,  $\ddot{\theta}$  is the

acceleration of the pitch angle,  $r$  is the distance between the motor and the center of gravity of the quadrotor and  $\tau_\theta$  is the pitch torque. So, the roll and pitch motion models can be simplified in Eqs. (31) and (32).

$$\ddot{\phi} = \frac{\tau_\phi}{I_{xx}} \quad (31)$$

$$\ddot{\theta} = \frac{\tau_\theta}{I_{yy}} \quad (32)$$

Then for the form of yaw rotational motion ( $\psi$ ) can be shown in Eq. (33), where  $I_{zz}$  is the quadrotor inertia on the z-axis,  $\ddot{\psi}$  is the yaw angular acceleration and  $\tau_\psi$  is the yaw torque.

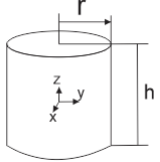
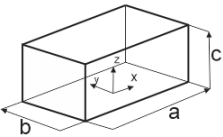
$$I_{zz} \cdot \ddot{\psi} = \sum_{i=1}^4 \tau_{M_i} \quad (33)$$

The yaw movement model does not use a thrust acting on the arm and motor but uses the torque resulting from the rotation of the motor at each end of the quadrotor arm so that the model can be simplified to Eq. (34).

$$\ddot{\psi} = \frac{\tau_\psi}{I_{zz}} \quad (34)$$

The quadrotor has a moment of inertia resulting from rotation on the x, y, and z axes. The Equation for the moment of inertia is adjusted to the shape of the component to be measured. There are two primary forms used to calculate the inertia of an object, namely the shape of a block or a cube and a cylinder. The equations used are in Table 1.

Table 1: Inertia equation [21]

Form	Image	Equation
Cylinder		$I_{G_{xx}} = I_{G_{yy}} = \frac{1}{12} m(3r^2 + h^2)$ $I_{G_{zz}} = \frac{1}{2} mr^2$
Solid Beams		$I_{G_{xx}} = \frac{1}{12} m(b^2 + c^2)$ $I_{G_{yy}} = \frac{1}{12} m(a^2 + c^2)$ $I_{G_{zz}} = \frac{1}{12} m(a^2 + b^2)$

### 3. CONTROL SYSTEM DESIGN

#### 3.1 Linear Quadratic Regulator (LQR) Control

LQR control is an optimal control that has a robust character and can produce a minimal steady-state error. This study utilizes LQR control with full state feedback gain. LQR control block diagram is interpreted in Fig. 2.

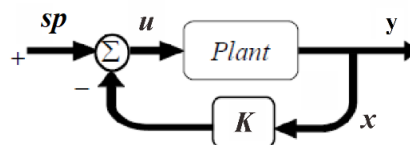


Fig. 2: LQR control diagram [18].



where  $sp$  is a reference or set point,  $u$  is control signal input,  $y$  is output signal,  $x$  is state control, and  $K$  is feedback gain. All components of LQR control are transformed in matrix dimension. The linear system equation in the LQR method is written through Eqs. (35) and (36) [19].

$$\dot{x} = Ax + Bu \quad (35)$$

$$y = Cx + Du \quad (36)$$

The cost function or index performance determines the performance of the LQR control. The best control signal performance is associated with the least possible yield weight. The formulation of the cost function is presented in Eq. (37) [19].

$$J = \int_{t_0}^{\infty} (x^T Qx + u^T Ru) dt \quad (37)$$

Based on Eq. (37), the control signal ( $u$ ) is generated from the control state's multiplication and the full state feedback gain. The control signal equation is shown in equation (38)[19].

$$u = -Kx \quad (38)$$

In the presence of Eq. (38), Eq. (35) will become Eq. (39) with the close-loop property in it.

$$\dot{x} = Ax - B(Kx) = (A - BK)x = A_c x \quad (38)$$

Also, by substituting Eq. (38) into Eq.(37), the cost function control equation will be,

$$J = \int_{t_0}^{\infty} (x^T Qx + K^T RK)x dt \quad (40)$$

The selection of the correct feedback value ( $K$ ) will result in optimal control. The accuracy of the  $K$  value is indicated by the performance value index or cost function  $J$  which is very minimal, close to 0. The performance index ( $J$ ) can be interpreted as a function of energy maintained at a small value in a closed-loop system. The performance index ( $J$ ) is weighted by state  $x(t)$  and the control input  $u(t)$ , where if  $J$  is minimized, state  $x(t)$  will go to zero for an infinite time that the closed-loop system will be stable.

The  $Q$  and  $R$  matrices are also influencing to performance of LQR control. Selecting the correct  $Q$  and  $R$  metrics will determine the best  $K$  feedback gain value for the system. The rule selection of matrices  $Q$  and  $R$  are as follows,

- The larger weight matrices  $Q$  will increase the value of gain feedback ( $K$ ), making a fast response system to achieve the intermediate state cost function.
- The larger weight matrices  $R$  will decrease the value of gain feedback ( $K$ ) which can slow down the steady-state (energy drive).

The optimal feedback gain  $K$  is found by deriving Eq. (40) using the Hamilton - Jacobi - Bellman method with proceed as follows.

$$\frac{d}{dt}(x^T Sx) = x^T (Q + K^T RK)x \quad (41)$$

$$J = \int_0^{\infty} \frac{d}{dt}(x^T Sx) dt = x^T(0)Sx(0) \quad (42)$$

where  $S$  is the auxiliary variable matrix. From Eq. (42), it is assumed that the closed-loop system is in a stable state with  $J$  being independent of the current  $K$  which depends on  $S$  and the initial conditions. By deriving and substituting Eq. (38) into Eq. (41), then,

$$\dot{x}^T Sx + x^T S\dot{x} + x^T Qx + x^T K^T RKx = 0 \quad (42)$$

$$x^T A_c^T Sx + x^T S A_c x + x^T Qx + x^T K^T RKx = 0 \quad (43)$$



$$x^T(A_c^T S + SA_c + Q + K^T RK)x = 0 \quad (44)$$

$$(A - BK)^T S + S(A - BK) + Q + K^T RK = 0 \quad (45)$$

$$A^T S + SA + Q + K^T RK - K^T B^T S - SBK = 0 \quad (46)$$

Based on Eq. (46), the feedback gain  $K$  is obtained by the following Eq. (47),

$$K = R^{-1}B^T S \quad (47)$$

with Eq. (46) solved by the Algebraic Riccati Equation (ARE). The equation for solving ARE can be seen in Eqs. (48) and (49) [19].

$$A^T S + SA + Q + (R^{-1}B^T S)^T R (R^{-1}B^T S) - (R^{-1}B^T S)^T B^T S - PB(R^{-1}B^T S) = 0 \quad (48)$$

$$A^T S + SA - SB R^{-1} B^T S + Q = 0 \quad (49)$$

### 3.2 Integral Control

Control of a closed-loop system using only proportional control or full state feedback control will almost certainly result in a steady-state error in the response for each system input. The steady-state error that occurs is called offset. The offset unit step is shown in Fig. 3.

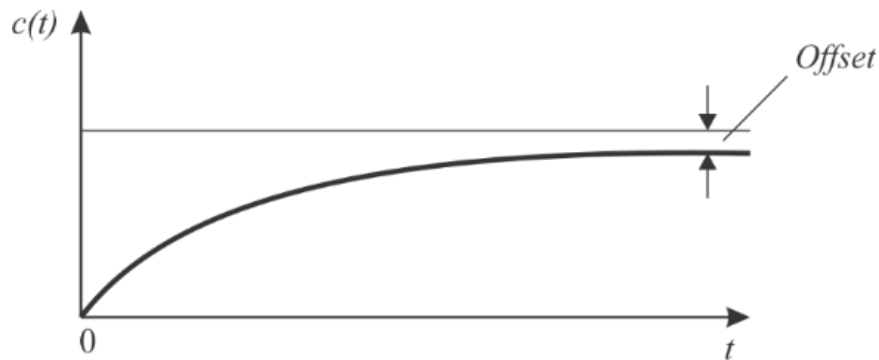


Fig. 3: Unit step response and offset [20].

The offset can be eliminated if integral control is added to the control system in controlling the system. Integral control has a functional equation described in Eq. (50)[20].

$$K_i = \int e(t)dt \quad (50)$$

### 3.3 LQR and Integrator Control Design on Quadrotor

A control system with a quadratic concept use 12 states as states obtained from quadrotor modelling. Based on Eqs. (17), (18), (19), (31), (32), and (33) are first converted into state-space, which refers to Eqs. (35) and (36). The basic concept of changing the form of a linear representation uses a system model with various orders spelt out into first-order orders. The shape of the quadrotor model state space is shown in Eq. (51) with the output signal—the form of state-space presented in Eq. (52).

$$\begin{bmatrix} \dot{x} \\ V_x \\ \dot{y} \\ V_y \\ \dot{z} \\ V_z \\ \dot{\phi} \\ \dot{\omega}_\phi \\ \dot{\theta} \\ \dot{\omega}_\theta \\ \dot{\psi} \\ \dot{\omega}_\psi \end{bmatrix} = \begin{bmatrix} 0 & 1 & 0 & 0 & 0 & 0 & 0 & 0 & 0 & 0 & 0 & 0 \\ 0 & 0 & 0 & 0 & 0 & 0 & 0 & 0 & -\frac{u_1}{m} & 0 & 0 & 0 \\ 0 & 0 & 0 & 1 & 0 & 0 & 0 & 0 & 0 & 0 & 0 & 0 \\ 0 & 0 & 0 & 0 & 0 & 0 & \frac{u_1}{m} & 0 & 0 & 0 & 0 & 0 \\ 0 & 0 & 0 & 0 & 0 & 1 & 0 & 0 & 0 & 0 & 0 & 0 \\ 0 & 0 & 0 & 0 & 0 & 0 & 0 & 0 & 0 & 0 & 0 & 0 \\ 0 & 0 & 0 & 0 & 0 & 0 & 0 & 1 & 0 & 0 & 0 & 0 \\ 0 & 0 & 0 & 0 & 0 & 0 & 0 & 0 & 0 & 0 & 0 & 0 \\ 0 & 0 & 0 & 0 & 0 & 0 & 0 & 0 & 0 & 1 & 0 & 0 \\ 0 & 0 & 0 & 0 & 0 & 0 & 0 & 0 & 0 & 0 & 0 & 0 \\ 0 & 0 & 0 & 0 & 0 & 0 & 0 & 0 & 0 & 0 & 0 & 1 \\ 0 & 0 & 0 & 0 & 0 & 0 & 0 & 0 & 0 & 0 & 0 & 0 \end{bmatrix} \begin{bmatrix} x \\ V_x \\ y \\ V_y \\ z \\ V_z \\ \phi \\ \omega_\phi \\ \theta \\ \omega_\theta \\ \psi \\ \omega_\psi \end{bmatrix} + \begin{bmatrix} 0 & 0 & 0 & 0 \\ 0 & 0 & 0 & 0 \\ 0 & 0 & 0 & 0 \\ 0 & 0 & 0 & 0 \\ 0 & 0 & 0 & 0 \\ -\frac{1}{m} & 0 & 0 & 0 \\ 0 & 0 & 0 & 0 \\ 0 & \frac{1}{I_{xx}} & 0 & 0 \\ 0 & 0 & 0 & 0 \\ 0 & 0 & \frac{1}{I_{yy}} & 0 \\ 0 & 0 & 0 & 0 \\ 0 & 0 & 0 & 0 \\ 0 & 0 & 0 & \frac{1}{I_{zz}} \end{bmatrix} \begin{bmatrix} u_1 \\ u_2 \\ u_3 \\ u_4 \end{bmatrix} \quad (51)$$

$$\begin{bmatrix} y_1 \\ y_2 \\ y_3 \\ y_4 \\ y_5 \\ y_6 \end{bmatrix} = \begin{bmatrix} 1 & 0 & 0 & 0 & 0 & 0 & 0 & 0 & 0 & 0 & 0 & 0 \\ 0 & 0 & 1 & 0 & 0 & 0 & 0 & 0 & 0 & 0 & 0 & 0 \\ 0 & 0 & 0 & 0 & 1 & 0 & 0 & 0 & 0 & 0 & 0 & 0 \\ 0 & 0 & 0 & 0 & 0 & 0 & 1 & 0 & 0 & 0 & 0 & 0 \\ 0 & 0 & 0 & 0 & 0 & 0 & 0 & 0 & 1 & 0 & 0 & 0 \\ 0 & 0 & 0 & 0 & 0 & 0 & 0 & 0 & 0 & 1 & 0 & 0 \end{bmatrix} \begin{bmatrix} x \\ V_x \\ y \\ V_y \\ z \\ V_z \\ \phi \\ \omega_\phi \\ \theta \\ \omega_\theta \\ \psi \\ \omega_\psi \end{bmatrix} + \begin{bmatrix} 0 & 0 & 0 & 0 \\ 0 & 0 & 0 & 0 \\ 0 & 0 & 0 & 0 \\ 0 & 0 & 0 & 0 \\ 0 & 0 & 0 & 0 \end{bmatrix} \begin{bmatrix} u_1 \\ u_2 \\ u_3 \\ u_4 \end{bmatrix} \quad (52)$$

where the inertia of the x, y, and z axes which are the components of Eq. (51), can be obtained by using reference Tabel 1 with Eqs. (53) to (55).

$$I_{xx} = \sum_{j=1}^n (I_{G_{xxj}} + m_j (y_j^2 + z_j^2)) \quad (53)$$

$$I_{yy} = \sum_{j=1}^n (I_{G_{yyj}} + m_j (x_j^2 + z_j^2)) \quad (54)$$

$$I_{zz} = \sum_{j=1}^n (I_{G_{zzj}} + m_j (x_j^2 + y_j^2)) \quad (55)$$

The LQR control method is specialized as a regulator. The problem that arises in this control system is when the user or the autonomous system wants to change the reference from the state. Changing the connection with a physical quantity of a state not equal to the input reference quantity can be done using the state reference ( $x_{ref}$ ).

Reference state can help maintain the vehicle's state with a specific position, such as an altitude position or translating the x and y axes of the Earth to a particular place. The existence of a reference state will modify Eqs. (35) to (56).

$$\dot{x} = Ax + B(-K(x - x_{ref})) \quad (56)$$

Based on Eq. (47), the calculation of the control signal ( $x - x_{ref}$ ) is an error against the desired reference, which is called an error. The error causes the system to produce a steady-state error or an offset against the reference or even more significant overshoot because the change in the value of the state changes directly, especially to maintain the translational motion of the x, y, and z axes of the vehicle to the Earth's axis. The calculation can be overcome by integrating the error and multiplied by a Gain. LQR control with a reference state is added to an Integrator component that converts Eq. (56) into Eq. (57).

$$\dot{x} = Ax + B(-K(x - x_{ref}) + K_i \int(x - x_{ref})) \quad (57)$$

This system has an  $A$  matrix system with 12x12 dimensions, a  $B$  matrix system with 12x4 dimensions, a  $C$  matrix system with 6x12 dimensions, the output signal ( $y$ ) in 6x1 dimension, and a control signal ( $u$ ) 12x1 matrix dimension. The control diagram design that interprets quadrotor control with state reference and Integral control is shown in Fig. 4.

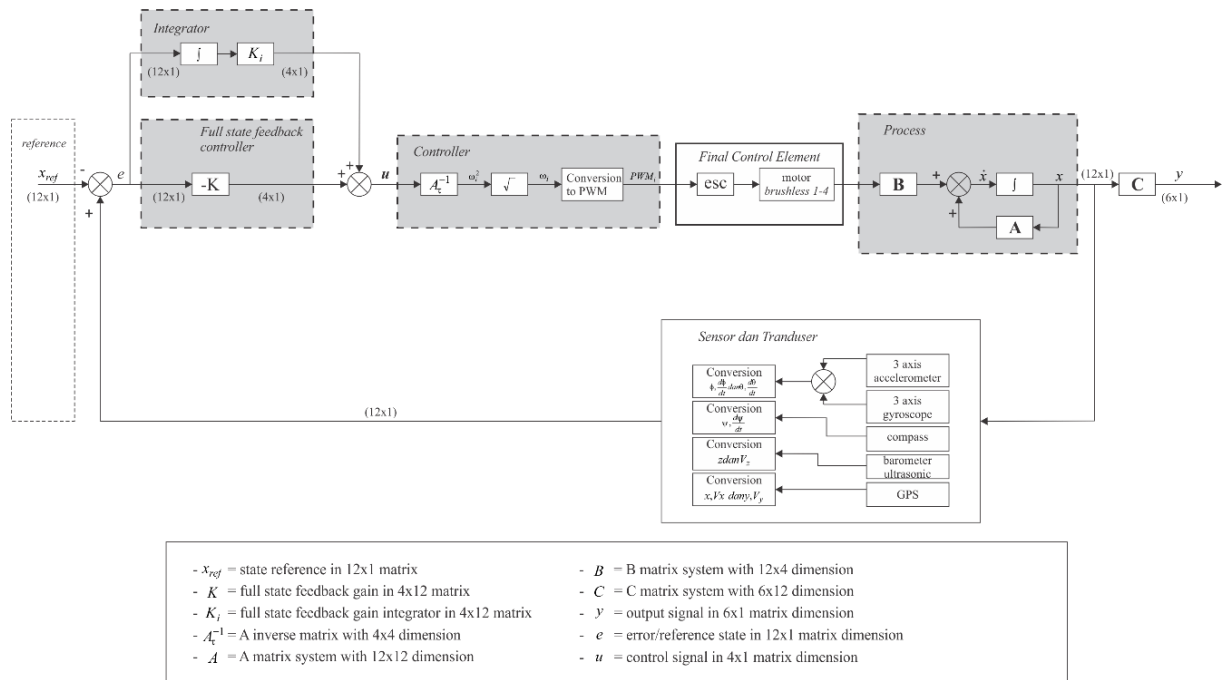


Fig. 4: LQR and Integrator control system on quadrotor.

Implementation of LQR Integrator control on quadrotor motion is based on the result of the integration of the dynamic equation. The force and torque on the quadrotor shown in Eq. (58).

$$\begin{bmatrix} F_T \\ \tau_\phi \\ \tau_\theta \\ \tau_\psi \end{bmatrix} = \begin{bmatrix} -b & -b & -b & -b \\ -lb & -lb & lb & lb \\ lb & -lb & -lb & lb \\ k & -k & k & -k \end{bmatrix} \begin{bmatrix} \omega_1^2 \\ \omega_2^2 \\ \omega_3^2 \\ \omega_4^2 \end{bmatrix} \quad (58)$$

where  $b$  and  $k$  are the coefficients of the thrust force and torque obtained from the calculation of Eqs. (59) and (60) [22].

$$b = C_T \rho A R_p^2 \quad (59)$$

$$k = C_q \rho A R_p^3 \quad (60)$$

where  $C_T$  and  $C_q$  are coefficients from propeller characteristics.  $\rho$  is the density of air, and  $A$  is the circle area of propeller and  $R_p$  is a radius of the propeller. The speed of each motor can be calculated through Eq. (61).

$$\begin{bmatrix} \omega_1^2 \\ \omega_2^2 \\ \omega_3^2 \\ \omega_4^2 \end{bmatrix} = A_z^{-1} \begin{bmatrix} F_T \\ \tau_\phi \\ \tau_\theta \\ \tau_\psi \end{bmatrix} = \begin{bmatrix} -b & -lb & lb & k \\ -b & -lb & -lb & -k \\ -b & lb & -lb & k \\ -b & lb & lb & -k \end{bmatrix} \begin{bmatrix} u_1 \\ u_2 \\ u_3 \\ u_4 \end{bmatrix} \quad (61)$$

#### 4. QUADROTOR MOVEMENT SCENARIO ON WAYPOINT TRACKING

Waypoint tracking flights require a structured and sequenced flight scenario to complete the mission. The quadrotor flight scenario in this study developed, which is described in Fig. 5.

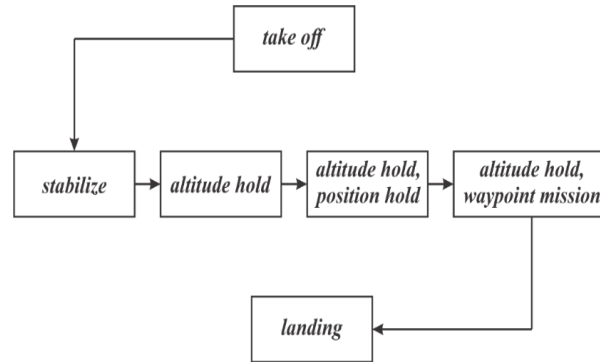


Fig. 5: Quadrotor movement scenario.

Quadrotor flying motion in tracing the waypoint trajectory is always set to move forward. This situation certainly causes the control of the x-axis translation of the quadrotor not only to utilize GPS latitude data, as well as the control of the y-axis translation of the quadrotor not only to utilize GPS longitude data. The quadrotor moves on the x-axis of the Earth. That refers to the longitude coordinates. It will rotate in front of the quadrotor, for example, 90°. The position makes the control of the quadrotor x-axis translation motion refer to latitude data. Figure 6 describes the quadrotor movement.

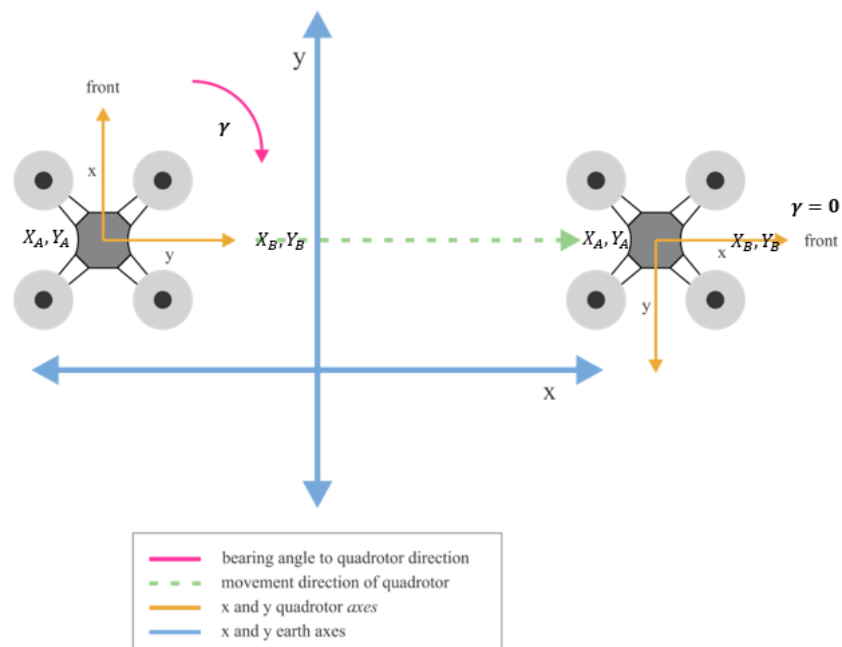


Fig. 6: Quadrotor direction to waypoint reference.

The rotation matrix concept solves the translational movement issue with the quadrotor's face. The face does not just face north, as indicated by the compass value of 0°. The rotation is centered on the z-axis and directed towards the quadrotor's x and y axes.

It is building a new axis based on the resulting angle. The new axis equation of the rotation matrix for the x and y axes is described by Eqs. (62) and (63).

$$X_A = X_B \cos \gamma - Y_B \sin \gamma \quad (62)$$

$$Y_A = X_B \sin \gamma + Y_B \cos \gamma \quad (63)$$

Another requirement for the quadrotor to constantly move forward when carrying out a search mission is adjusting the quadrotor from the current coordinate point to the intended waypoint coordinates. This adjustment is in the form of a calculation angle from two different coordinate points as the reference state yaw value. The calculated angle is called the bearing angle. The position of the angle is shown in Fig. 7 [16].

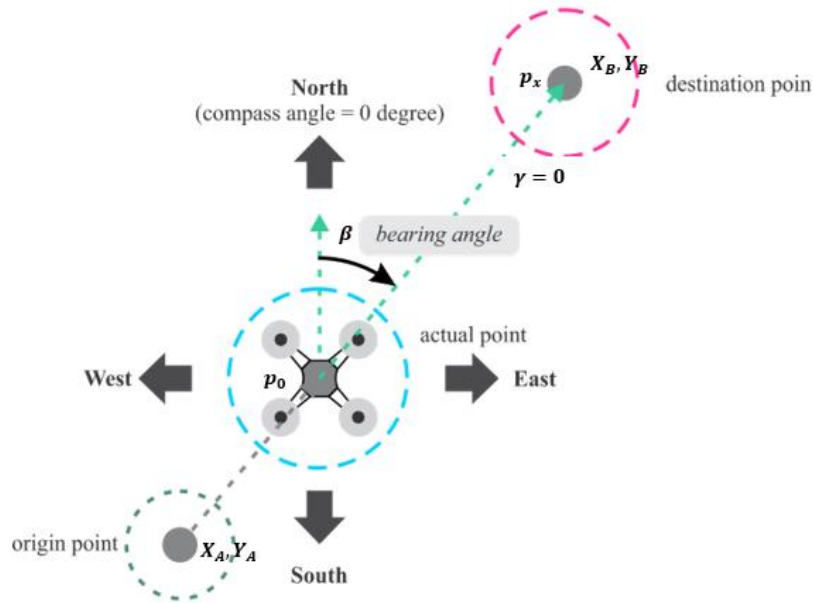


Fig. 7: Bearing angle from two difference of coordinate point location.

The bearing angle ( $\beta$ ) is based on taking the compass angle value of  $0^\circ$  with the magnetic north of Earth. This angle ( $\beta$ ) is obtained from two positions of latitude ( $\varphi$ ) and longitude ( $\lambda$ ) measures of the GPS coordinate frame. Two coordinate points meant are the actual point of the quadrotor in any position during flight and destination point. The actual point is represented by the longitude and latitude of GPS coordinate with  $p_0$  symbol. On the other hand, the destination point is represented by the longitude and latitude of the following planning position coordinate with  $p_x$  symbol. Updating bearing angel can be calculated by the Haversine formula, where the first step is found longitude distance ( $\delta_\lambda$ ) between  $p_0$  and  $p_x$  in radians units. The longitude distance can be processed as follows [16],

$$\delta_\lambda = (\lambda_{p_0} - \lambda_{p_x}) \quad (64)$$

Different longitude distance is then converted from degree to radians as follows in Eq. (65).

$$\delta_\lambda = (\lambda_{p_0} - \lambda_{p_x}) * \frac{180}{\pi} \quad (65)$$

We know if Earth has a round form with 3 Dimension perspective. So the Haversine formula should be implemented in this calculation to obtain accurate information. Therefore, Eq. (66) is described using a formula,

$$a_\lambda = \sin(\delta_\lambda) * \cos\left(\varphi_{p_x} * \frac{180}{\pi}\right) \quad (66)$$

This process also applies to latitude coordinates that can be described by Eqs. (67) and (68).

$$a_{\varphi_1} = \sin\left(\varphi_{p_0} * \frac{180}{\pi}\right) * \cos\left(\varphi_{p_x} * \frac{180}{\pi}\right) \cos(\delta_\lambda) \quad (67)$$

$$a_{\varphi_2} = \cos\left(\varphi_{p_0} * \frac{180}{\pi}\right) * \sin\left(\varphi_{p_x} * \frac{180}{\pi}\right) - a_{\varphi_1} \quad (68)$$

Based on the relation of longitude and latitude in the radians unit, the bearing angel ( $\beta$ ) can be calculated in degree unit using Eq. (69).

$$\beta = atan2(a_\lambda, a_{\varphi_2}) \quad (69)$$

## 5. ARCHITECTURE SYSTEMS

### 5.1 Electronic Design System

Input from the quadrotor system in several sensors measuring data is the design's value, especially in the quadrotor control system. The sensors are an accelerometer and a gyroscope that produce data in the form of roll angle and pitch values from the sensor fusion process using the DMP method. Yaw angle data is obtained from the compass sensor.

The following sensors are barometer and ultrasonic, which are used to provide altitude data. The barometer sensor is used when the quadrotor flies above one meter. The pressure data is filtered and converted to altitude using the SISO Kalman filter.

Then the U-block LEA-6H module GPS sensor is used with an accuracy of up to 0.010. This sensor provides longitude and latitude data which is converted into meters. Also, this sensor acts as quadrotor control data in maintaining position and as a control in tracking the waypoint path. Like the barometer, this sensor also experiences drifting, especially for readings of the Earth's longitude, requiring data filtering first. The Kalman filter also uses the method of filtering GPS data. The hardware used in processing the algorithm in this study is an ARM Cortex-M4 microcontroller with a computational speed of 96 MHz and rated speed which can be increased through overclocking up to 120 MHz.

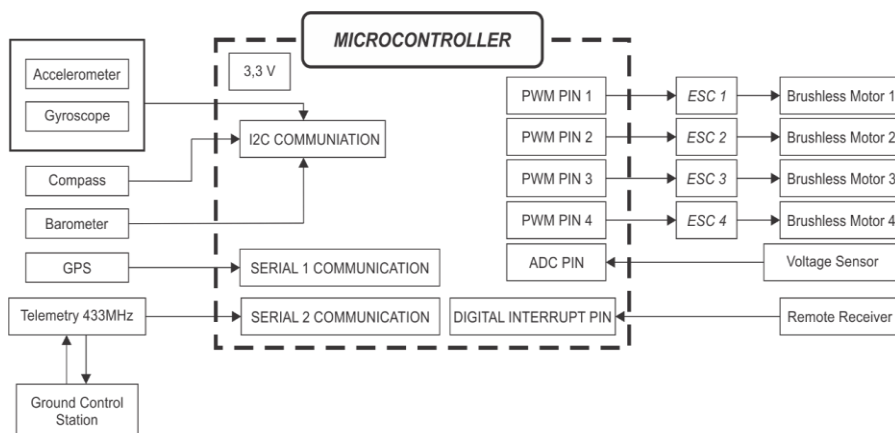


Fig. 8: Electronics architecture of quadrotor.

The last part of the electronic device system is the output part. This section is an actuator to drive the speed and direction of flight of the quadrotor. The electronic hardware used is a brushless motor with a specification of 980 kV. The engine is a three-

phase DC motor controlled using an electronic speed controller module that pulses from the microcontroller PWM port. This motor uses a propeller 10 x 4.5. The relation of the three electronic hardware is shown in Fig. 8.

## 5.2 Mechanical Design

This mechanical frame consists of an upper center plate, lower center plate, and four arms attached to the sides of the center plate. Between the upper and lower center plates, space is occupied by a battery in the form of a sized block and a telemetry module. The top center plate is used to place the microcontroller shield and the GPS buffer antenna, and the GPS module itself. Another part of the frame is the arm. It is used as the 980 kV brushless motor placement with a 10 x 5 propeller HQ-prop type and ESC. The mechanics of the aircraft spacecraft are shown in Fig. 9 and Fig. 10.



Fig. 9: Mechanics design of quadrotor in top view.

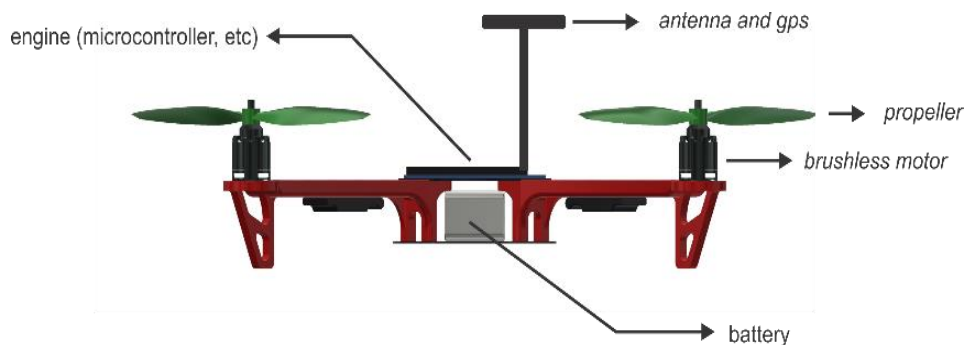


Fig. 10: Mechanics design of quadrotor inside view.

## 5.3 Flow Concept Programming

The main program of the Quadrotor system starts by declaring the header and several libraries used, then declarations of variables needed in the system. Furthermore, the system will enter into a setup condition, where this section is the initial condition of the sensor access, telemetry, remote reading receiver, and actuator. After the program enters the setup section, the program will enter the loop function. This function is a function that will run the program repeatedly until the system is disabled. In this function, the system will check the condition of getting flight orders or not. When the system conditions are changed into flight commands, the system will take raw data from the sensors, where the



sensor data is processed and acquired through the filtering and sensor fusion processing sub-functions. Then the program will operate the rotational motion correction function, namely flight control, by maintaining the quadrotor rotational attitude using the LQR and Integrator control system control. The flow of the main algorithm is shown in Fig. 11.

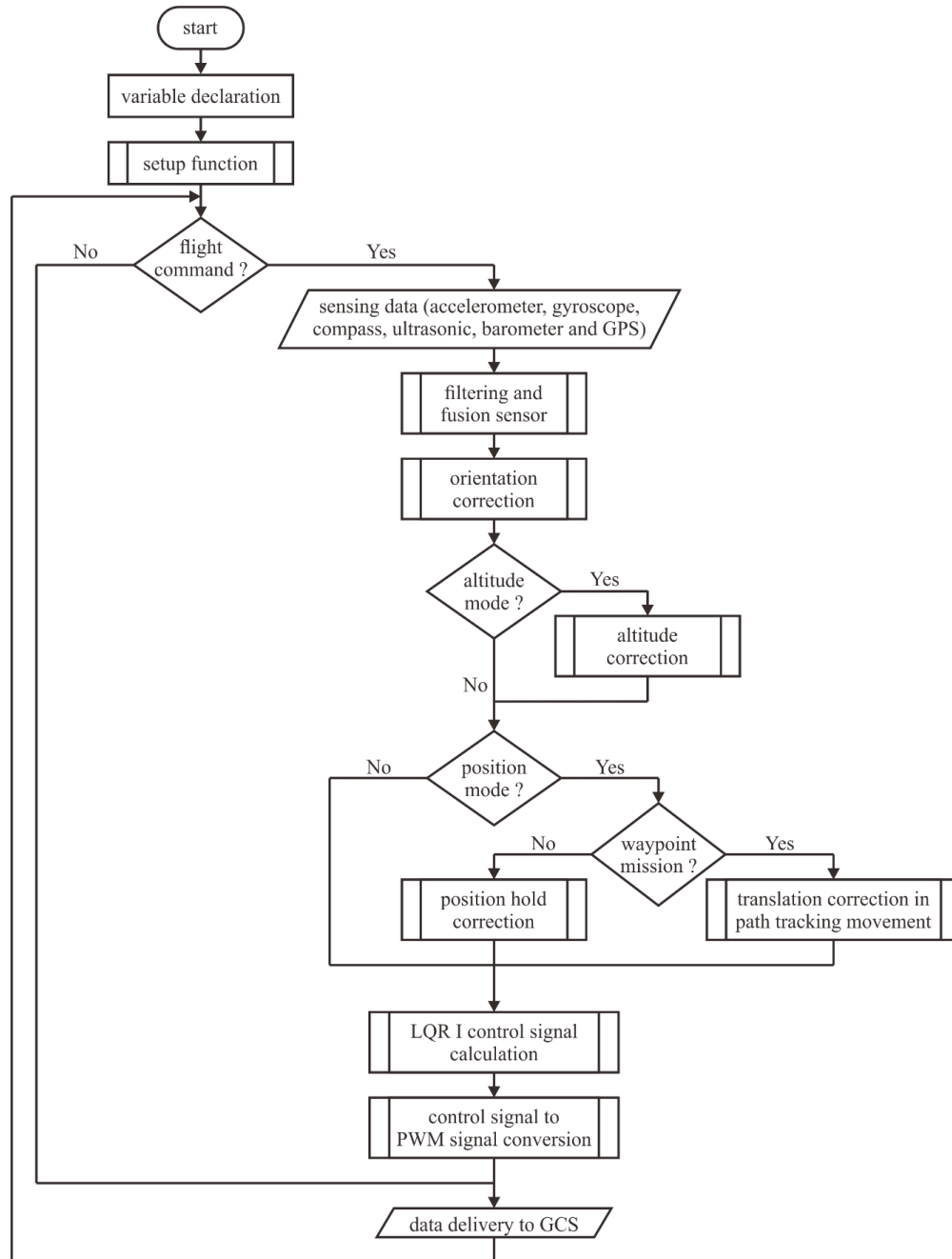


Fig. 11: Main flow diagram of a quadrotor system.

## 6. RESULTS AND DISCUSSION

Based on the flight scenario that has been designed, it is necessary to test and analyze the characteristics of the quadrotor. Observations were made at the point of maintaining anti-rotational motion, maintaining altitude, maintaining the anti-translational motion of the x and y axes, and defending the waypoint path. This stability test refers to the plane parameters calculated physically and mathematically, as shown in Table 2.

Table 2: Parameters of quadrotor

Parameter	Value	Unit
$C_T$	$1.915 \times 10^{-4}$	-
$C_Q$	$1.830 \times 10^{-5}$	-
$R$	$1.250 \times 10^{-1}$	m
$\rho$	1.184	kg.m <sup>3</sup>
$A$	$4.910 \times 10^{-2}$	m <sup>2</sup>
$I_{xx}$	$1.320 \times 10^{-2}$	kg.m <sup>2</sup>
$I_{yy}$	$1.402 \times 10^{-2}$	kg.m <sup>2</sup>
$I_{zz}$	$1.237 \times 10^{-2}$	kg.m <sup>2</sup>
$b$	$1.739 \times 10^{-7}$	-
$k$	$1.229 \times 10^{-9}$	-

Based on the experiments, it is found that the movement attitudes have increased stability with integrator control. The stability is obtained by determining the full state feedback constant value  $K$  and  $K_i$  of each quadrotor state. The constants are influenced by the weighting of the  $Q$  and  $R$  elements [23]. The greater weighting of the  $Q$  element will result in a more significant gain value  $K$  as well. The greater the gain value  $K$ , the greater the torque on the quadrotor system, making the system more responsive than giving a small gain value  $K$  [24]. The best correlation constants with  $Q$  and  $R$  quadrotor in this study are shown in Tables 3 and 4.

Table 3: Conversion matrix of  $Q$  element to gain  $K$  on quadrotor

$Q$	$R$	$K$
$\begin{bmatrix} 0.87 & 0 & 0 & 0 & 0 & 0 & 0 & 0 & 0 & 0 & 0 & 0 & 0 \\ 0 & 124.6 & 0 & 0 & 0 & 0 & 0 & 0 & 0 & 0 & 0 & 0 & 0 \\ 0 & 0 & 1.77 & 0 & 0 & 0 & 0 & 0 & 0 & 0 & 0 & 0 & 0 \\ 0 & 0 & 0 & 124.6 & 0 & 0 & 0 & 0 & 0 & 0 & 0 & 0 & 0 \\ 0 & 0 & 0 & 0 & 178.3 & 0 & 0 & 0 & 0 & 0 & 0 & 0 & 0 \\ 0 & 0 & 0 & 0 & 0 & 1955.9 & 0 & 0 & 0 & 0 & 0 & 0 & 0 \\ 0 & 0 & 0 & 0 & 0 & 0 & 1.73 & 0 & 0 & 0 & 0 & 0 & 0 \\ 0 & 0 & 0 & 0 & 0 & 0 & 0 & 6.89 & 0 & 0 & 0 & 0 & 0 \\ 0 & 0 & 0 & 0 & 0 & 0 & 0 & 0 & 2.95 & 0 & 0 & 0 & 0 \\ 0 & 0 & 0 & 0 & 0 & 0 & 0 & 0 & 0 & 325.5 & 0 & 0 & 0 \\ 0 & 0 & 0 & 0 & 0 & 0 & 0 & 0 & 0 & 0 & 4.81 & 0 & 0 \\ 0 & 0 & 0 & 0 & 0 & 0 & 0 & 0 & 0 & 0 & 0 & 168.6 & 0 \end{bmatrix}$	1	$\begin{bmatrix} 0 & 0 & 0 & 0 & 13.35 & 44.61 & 0 & 0 & 0 & 0 & 0 & 0 & 0 \\ 0 & 0 & 1.33 & 11.67 & 0 & 0 & 1.32 & 2.63 & 0 & 0 & 0 & 0 & 0 \\ 0.93 & 11.67 & 0 & 0 & 0 & 0 & 0 & 0 & 1.72 & 18.07 & 0 & 0 & 0 \\ 0 & 0 & 0 & 0 & 0 & 0 & 0 & 0 & 0 & 0 & 2.19 & 12.99 & 0 \end{bmatrix}$

Table 4: Integrator constant ( $K_i$ ) matrix on quadrotor

$K_i$
$\begin{bmatrix} 0 & 0 & 0 & 0 & 0.04 & 0 & 0 & 0 & 0 & 0 & 0 & 0 & 0 \\ 0 & 0 & 0.002 & 0 & 0 & 0 & 0.0053 & 0.0008 & 0 & 0 & 0 & 0 & 0 \\ 0.004 & 0 & 0 & 0 & 0 & 0 & 0 & 0 & 0.004 & 0.0011 & 0 & 0 & 0 \\ 0 & 0 & 0 & 0 & 0 & 0 & 0 & 0 & 0 & 0 & 0 & 0.005 & 0 \end{bmatrix}$

As a starting point, the  $Q$  for each observed state is the value 1. Then the  $Q$  value approach is carried out in getting the best feedback gain system response through trial error and graphical analysis. Meanwhile, the value of  $R$  is set at 1 for all states.

The results of testing each quadrotor state that has been carried out are described in the following sub-sections.

## 6.1 Rotation Movement Characteristics Stability

Testing of roll, pitch, and yaw rotational motion is carried out by giving a range of 20 degrees counterclockwise deviations for state roll and pitch and 20 degrees clockwise for state yaw. The test was applied to 5 experiments with a period of 9 seconds. From the testing process, the characteristics response of each rotation is shown in Table 5 for roll response, Table 6 for pitch response and Table 7 for yaw response.

Table 5: Roll rotation stability response

Response Transient	Test 1	Test 2	Test 3	Test 4	Test 5	Average	Requirement System
Rise Time (tr) →	0.24	1.54	<b>0.19</b>	0.27	0.18	0.65	< 1 seconds
Settling time (ts) →	2	1.4	<b>1.5</b>	1.5	2.6	1.48	< 3 seconds
Overshoot →	3.22	0	<b>3.92</b>	4.38	6.8	3.66	< 9 degrees
Undershoot →	-2.11	-3.82	<b>0</b>	-2.96	-4.11	2.6	> -9 degrees
Steady State Error →	0.85	0.02	<b>-0.02</b>	0.38	0.01	0.25	± 4.5 degrees

Table 6: Pitch rotation stability response

Response Transient	Test 1	Test 2	Test 3	Test 4	Test 5	Average	Requirement System
Rise Time (tr) →	0.32	<b>0.48</b>	0.47	0.35	0.16	0.37	< 1 seconds
Settling time (ts) →	2.3	<b>0.9</b>	1.7	1.8	2.8	1.9	< 3 seconds
Overshoot →	4.72	<b>1.77</b>	4.76	2.71	4.71	3.73	< 9 degrees
Undershoot →	-2.57	<b>0</b>	0	-3.11	-4.74	2.08	> -9 degrees
Steady State Error →	0.69	<b>-0.46</b>	0.04	-0.61	0.06	-0.06	± 4.5 degrees

Table 7: Yaw rotation stability response

Response Transient	Test 1	Test 2	Test 3	Test 4	Test 5	Average	Requirement System
Rise Time (tr) →	1.45	4.71	0.84	<b>0.96</b>	0.83	1.76	< 1 seconds
Settling time (ts) →	4.6	4.90	4.7	<b>2.5</b>	4.3	4.2	< 3 seconds
Overshoot →	0	0	0	<b>0</b>	5.23	1.02	< 9 degrees
Undershoot →	-8.91	0	-8.59	<b>-1.28</b>	0	3.76	> -9 degrees
Steady State Error →	-0.88	-0.55	-1.67	<b>0.80</b>	-3.16	-1.09	± 4.5 degrees

Based on Tables 5 to 7, state roll, pitch, and yaw with LQR and Integrator control for the entire trial of five times, the quadrotor has response characteristics that meet the minimum specifications for system stability. The best response attitude results in the third test for the state roll. The third test results only have an overshoot of 3.92 degrees and no undershoot. The rise time and settling time in the third test results are among the fastest in stabilizing the system, namely 0.19 seconds and 1.5 seconds. This test also produces a minimum steady-state error of 0.02 degrees compared to other test results. While the best result for pitch is the second test and the fourth test for the yaw state. The three best responses are the results of the analysis of the flight data plots shown in Figs. 12 to 14.

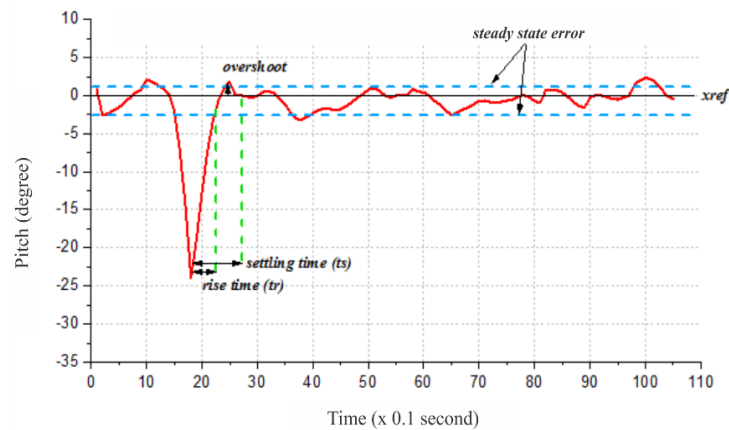


Fig. 12: Pitch angle rotation response.

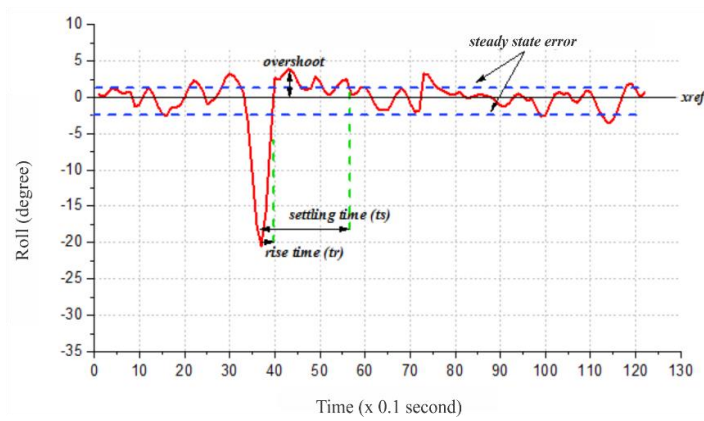


Fig. 13: Roll angle rotation response.

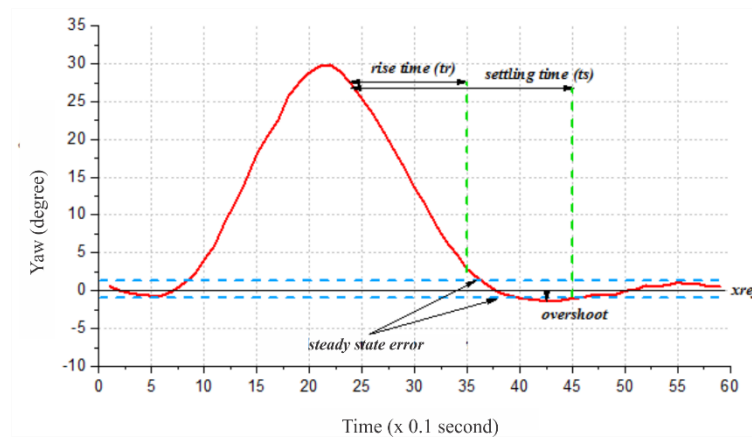


Fig. 14: Yaw angle rotation response.

Tests conducted on the three states prove that the LQR control with the addition of an Integrator can maintain the torsional stability of both roll, pitch, and yaw against disturbances that only require minimal potential energy. Besides, the short response speed of the test results indicates the need for a small cost function to stabilize the roll rotation motion [25].

On the other hand, there is a significant difference in rising time, settling time, overshooting, and undershooting the yaw state control analysis. The yaw angle data still fluctuates even though it has gone through compensation and data filtering stages.

Fluctuations occur because the magnetometer sensor's readings are influenced by the magnetic field around the sensor and the Earth's magnetic field [26]. Even so, the system is still able to accommodate a quadrotor to fly to control the yaw torque with good stability specifications.

## 6.2 Altitude Response Stability

Control in maintaining altitude controls the vertical axis  $z$  quadrotor translational motion associated with a thrust. This study utilizes data from the barometer and ultrasonic sensors to obtain elevation values above the ground as a controlled state.

The weighting mechanism of the  $Q_z$  and  $Q_{V_z}$  Elements in the LQR control start from a value of 1, which is then added and subtracted to get a  $K$  gain that meets the system requirements. In contrast, the Integrator  $K_i$  gain is tuned from the smallest possible value starting with one 100 of the best  $K$  LQR value. The bigger of the Integrator will provide a response strength that can cause rapid oscillation [27].

To analyze the response of the quadrotor system in altitude maintenance. The test set off altitude flight of quadrotor in 75 cm, giving some disturbance in the form of a deviation in the range of 25 cm towards the ground surface. The results of these tests are interpreted through the analysis of the response characteristics of the altitude hold motion shown in Table 8.

Table 8: Altitude hold stability response

Response Transient	Test 1	Test 2	Test 3	Test 4	Test 5	Average	Requirement System
Rise Time (tr) →	0.75	0.76	<b>0.83</b>	0.96	1.17	0.89	< 3 seconds
Settling time (ts) →	3.8	4.6	<b>2.7</b>	3.3	3.7	3.62	< 6 seconds
Overshoot →	0.07	0.03	<b>0.03</b>	0.07	0.03	0.04	≤ 0.07 meters
Undershoot →	0	-0.02	<b>0</b>	0	0	0.004	≥ -0.07 meters
Steady State Error →	-0.02	-0.01	<b>-0.02</b>	0.02	0.01	-0.004	± 0.0375 meters

The best characteristics of the aircraft are obtained when the third test. The resulting test only has a minimum overshoot of 0.03 degrees and no undershoot in the system. Furthermore, the system has the fastest settling time than others. This test also produces a minimum steady-state error of -0.02 degrees. The characteristic is carried out, shown by the flight data plotting, as shown in Fig. 15.

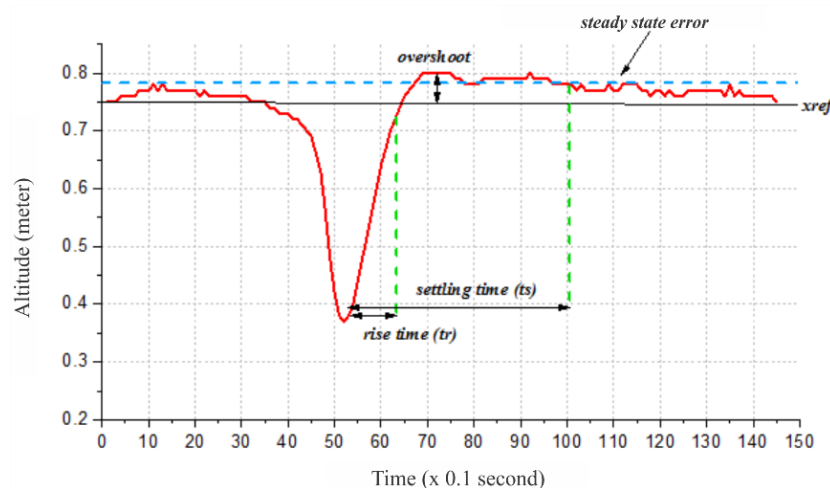


Fig. 15: Altitude hold response.

The characteristics of the quadrotor have a settling time for each test, having a relatively slow time and minimal undershoot in reaching a steady state. This condition is caused by updating the vertical translation speed state, which is longer, and using a considerable gain value so that the quadrotor will slowly hold the momentum after the overshoot occurs.

Testing is also carried out by varying the reference height to find out more characteristics. The variation in altitude is adjusted to the reference height of 1.8 m, 3.4 m, and 4.8 m by utilizing the height data from the barometer sensor. The results of the flight test are depicted in Fig. 16.

The calculation result of the steady-state error is -0.0131 m for a height of 1.8 m, -0.0283 m for a height of 3.4 m, and 0.025 m for a height of 4.8 m. A minor steady-state error generated at the lowest altitude does not mean that the system has the minimum error. The system is steady-state with the slightest inclination interval, namely the range  $\pm 0.02$  m, namely at an altitude of 4.8 m. The barometer sensor readings are accurate at higher altitudes.

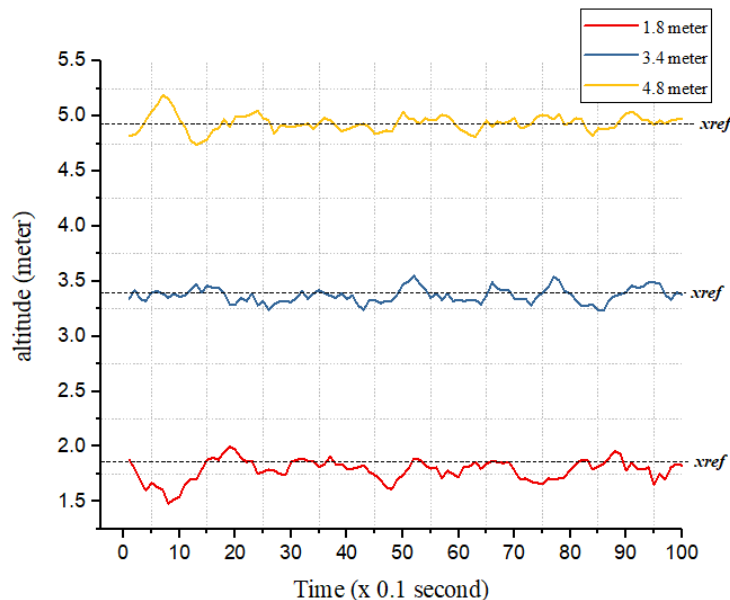


Fig. 16: Altitude hold response in different reference of high.

However, the LQR control system with the addition of the Integrator concept as compensation can be appropriately controlled by meeting the system requirements specification. The steady-state error occurs no more than 10% of the reference altitude.

### 6.3 Translation Movement Characteristics Stability

This test is categorized into two segments: translational motion, maintaining absolute earth coordinates, and translational motion when performing a waypoint mission.

#### 6.3.1 Position Hold Stability

In principle, a horizontal translational motion has two controlled x and y axes. Control of horizontal quadrotor translation motion depends on the accuracy of using the Global Positioning System sensor to obtain data in the form of displacement state and x-axis translation speed from longitude data conversion and y-axis data from latitude data conversion. Referring to previous research conducted by [28], giving a tolerance limit of

2.5 m to the front, back, right, and left of the quadrotor. The quadrotor translation motion test is analyzed based on comparing the use of the LQR and LQR Integrator controls.

This part of the translational motion trial was carried out five times without getting disturbed by the current environmental conditions. Based on the five tests, the quadrotor has flight characteristics in maintaining the x-axis and y-axis positions as described in Tables 9 and 10.

Table 9: Comparison of x-axis translation stability using LQR and LQR Integrator

Control Method	Error Properties	Test 1	Test 2	Test 3	Test 4	Test 5	Average
LQR	Max. deviation (meters)	2.71	2.74	3.23	1.78	3.15	2.72
	Min. deviation (meters)	-2.63	0.40	-1.14	1.69	0.22	-0.29
	Steady state error (meters)	0.12	1.84	0.93	-0.06	1.91	0.95
LQR Integrator	Max. deviation (meters)	0.41	0.39	1.49	0.14	0.74	0.63
	Min. deviation (meters)	-1.35	-1.04	-0.12	-1.36	-1.49	-1.07
	Steady state error (meters)	0.10	-0.35	0.55	-0.72	-0.36	-0.15

Table 10: Comparison of y-axis translation stability using LQR and LQR Integrator

Control Method	Error Properties	Test 1	Test 2	Test 3	Test 4	Test 5	Average
LQR	Max. deviation (meters)	3.21	-0.03	0.14	4.09	4.96	2.47
	Min. deviation (meters)	0.80	-1.93	-2.99	0.57	0.48	-0.61
	Steady state error (meters)	2.07	-1.19	-1.36	2.45	2.10	0.82
LQR Integrator	Max. deviation (meters)	0.40	1.95	2.28	1.98	2.27	1.52
	Min. deviation (meters)	0.47	2.19	-1.96	-1.52	-1.79	-0.52
	Steady state error (meters)	-0.28	0.21	-0.51	-0.70	0.98	-0.06

The results also prove, by using the LQR control coupled with Integral. It can give a quadrotor translation motion system needed. The error calculation of a steady-state error has an average of -0.06 meters for the x-axis and -0.15 meters for the y-axis. On the other hand, the steady state error using the LQR control produces a more considerable error with an average of 0.95 for the x-axis and 0.82 for the y-axis. The accuracy and precision of the control process can be seen in Table 11.

Table 11: Comparison between LQR and LQR Integrator method in position hold stabilization of a quadrotor

Control Method	Parameter	Test 1	Test 2	Test 3	Test 4	Test 5	Average
LQR	Accuracy in %	62	90	80	66	58.67	71.33
	Precision in %	23.81	30.18	45.89	32.84	46.82	35.91
LQR Integrator	Accuracy in %	100	100	100	100	100	100
	Precision in %	45.45	35	38.62	37.93	31.54	37.71

Accuracy and precision are evidenced in Fig. 17, which compares the distribution of quadrotor data with LQR and LQR and Integrator.



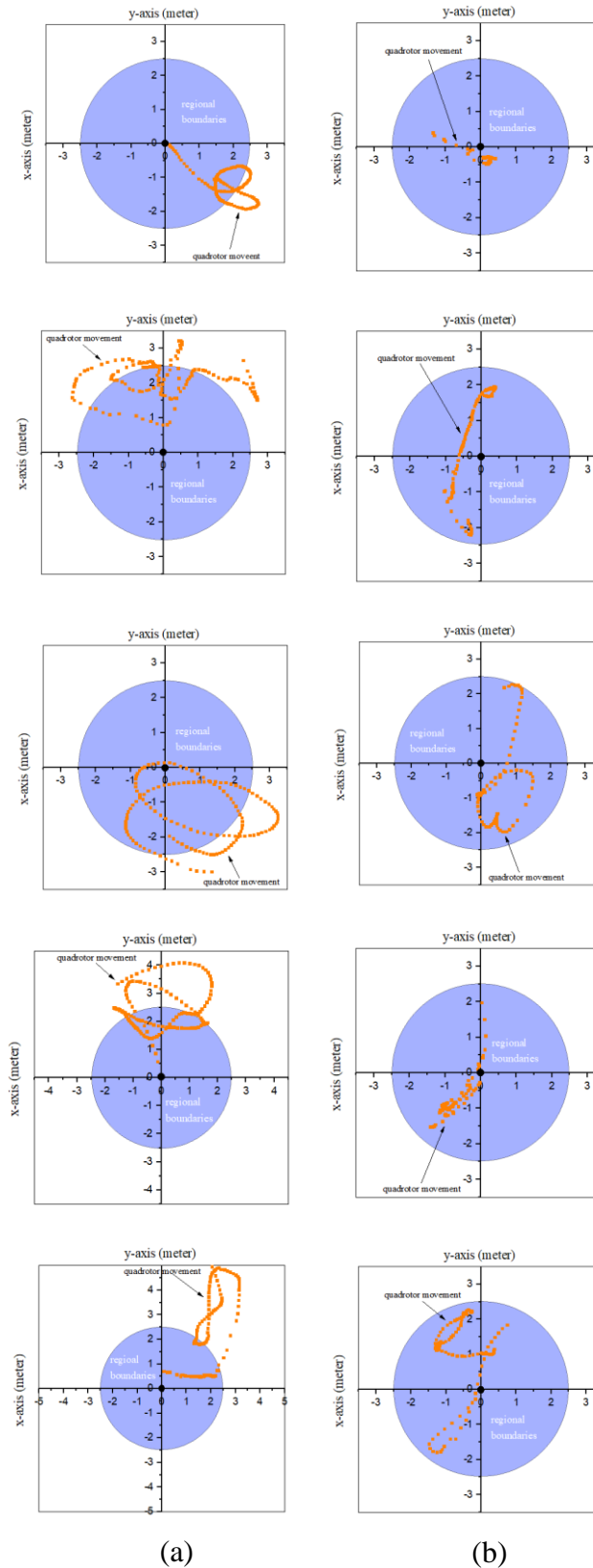


Fig. 17: Quadrotor position hold movement using (a) LQR control (b) LQR Integrator control.

The accuracy is calculated from a division of the number data in the tolerance limit (the light blue circle) by a value of 150 and multiplied by 100%. It can be written into the following Eq. (70) form,

$$Accuracy = \frac{\text{Number of data in limit tolerance}}{150} \times 100\% \quad (70)$$

The number 150 comes from taking flight data from the quadrotor test, where each flight is carried out for 15 seconds and produces 150 data. The calculation results prove that using LQR and Integrator control as a quadrotor control system can increase the accuracy to 100% from 71.33% accuracy of LQR control accommodation only. The LQR and Integrator control making the quadrotor system only requires less energy than the LQR control.

High accuracy does not necessarily have high precision either. The precision itself is the closeness of the difference in the value of each data distribution from a data set. In the case of anti-translational motion control, the precision given to the LQR and Integrator control on the system is not so significant, which only increases the range of 1.8% of the LQR control. The compensation of Integrator does have properties that increase the system's responsiveness. So, the quadrotor error can be reduced, but it is not meaningful with good damping properties.

Meanwhile, the precision value is obtained from the calculation step of the average of each position distance to the reference and the standard deviation, where one data is represented by two displacement data x and y with displacement references x and y equal to zero. Then the distance of a position point to the reference point can be calculated using the Pythagoras formula, such as Eq. (71):

$$\text{range position to the reference} = \sqrt{x^2 + y^2} \quad (71)$$

The precision of each distance as a ratio of the standard deviation against the average of range postopn to the reference multiplied by 100%, as in Eq. (72),

$$Precision = \frac{\text{deviation standar of rage position to the refernce}}{\text{average of range position to the reference}} \times 100\% \quad (72)$$

### 6.3.2 Translation Stability in Waypoint Mission

The control system testing on translational movement when tracing a path is applied to a different path pattern. The track pattern consists of squares and zig-zags. The box waypoint trajectory pattern is constructed by entering four different latitude and longitude coordinates, where the coordinates of the points are shown in sequence in Table 12.

Table 12: Coordinate trajectory pattern of waypoint

State Coordinate of waypoint	Square Pattern		Zig-zag Pattern	
	Latitude	Longitude	Latitude	Longitude
1	-7.751096	110.348807	-7.751096	110.348807
2	-7.750976	110.348807	-7.751096	110.348927
3	-7.750976	110.348927	-7.750976	110.348807
4	-7.751096	110.348927	-7.750976	110.348927

These coordinate points are determined based on satellite image data on one of the features provided by Google Earth by forming the path of each flight trajectory pattern as shown in Fig.18 (a, b).

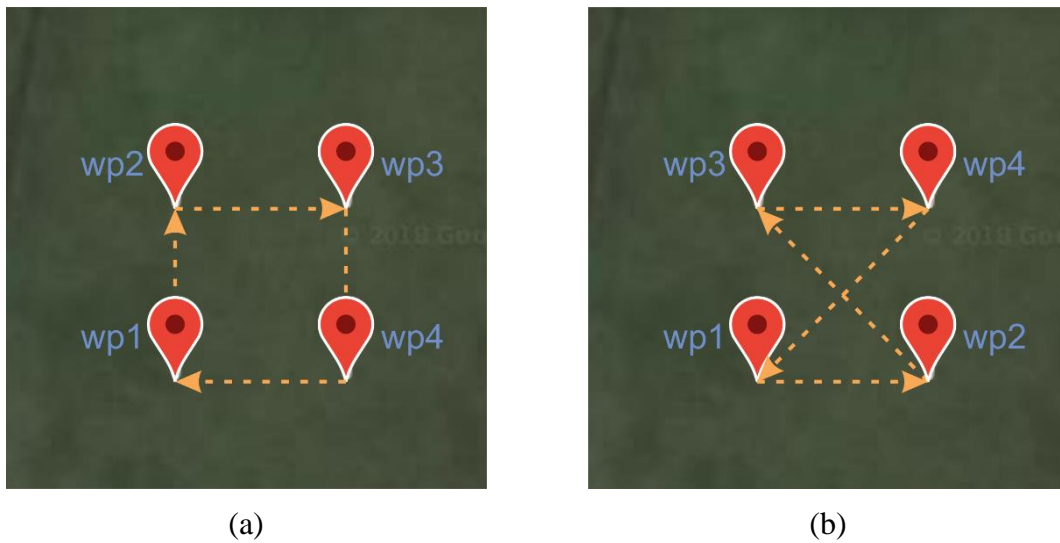


Fig. 18: Waypoint flow movement of the quadrotor in (a) square and (b) zig-zag trajectory pattern.

The basic concept of this translational motion control system analysis is carried out in the movement of the x-axis or lateral axis of the aircraft. The velocity of the quadrotor becomes one of the determining factors for the success of the quadrotor in the waypoint mission. The velocity will generate momentum in the plane, which makes it unable to defend stabilization. The correct value of velocity in a waypoint mission flight will make the quadrotor fly more accurate towards the right path [29]. Therefore, this study varies the speed of the quadrotor in each flight mission in tracing the trajectory with three-speed variations that can minimize the percentage of flight errors or errors, as explained in Table 13.

Table 13: Quadrotor flight velocity variation to the performance of trajectory error

Trajectory Pattern	Velocity ( $\frac{m}{s}$ )	Range (m)	% Error
Square	0.5	52	37.78
	1	52	5.04
	1.5	52	68.89
Zig-zag	0.5	62.76	37.83
	1	62.76	13.51
	1.5	62.76	66.72

The error presentation reflects the accuracy of the quadrotor to be traced in the path. The error presentation is calculated from the position based on the fault tolerance limit during the flight mission. Error calculation can be calculated using Eq. (73),

$$\% \text{ Error} = \frac{\text{The amount of quadrotor position data is out of tolerance}}{\text{Total of data recording in waypoint mission}} \times 100\% \quad (73)$$

From the results of data processing, it was found that the slightest error percentage in both in box and zig-zag trajectory occurred in the quadrotor system with a flight speed of 1 m / s. In comparison, the most significant error happened when the quadrotor speed was set at 1.5 m / s with an error percentage of 68.89% for the square track pattern and 66.72%

for the zig-zag trajectory. A higher velocity than the system requirement will produce a steady-state that is out of the path tolerance limit. It happened because lateral motion control requires navigation data to run slower in correcting errors. Also, the high velocity can make overshoot component on the flight of a quadrotor. Overshoot occurs because the process of moving the quadrotor movement moves forward towards a stop condition when it enters the waypoint point to change the direction of a quadrotor. In this situation will be tremendous momentum so that the plane is likely to bounce.

The low speed of the system requirements will also affect the number of errors that occur, although not as large as the errors generated at high-speed settings. The percentage of error was 37.78% in the square track pattern and 37.83% in a zig-zag way for the velocity of  $0.5 \frac{m}{s}$ . The velocity is set lower than the system requirement. It will make the aircraft character less able to correct the drift that occurs. Resulting in the quadrotor to produce track tracking movements still with errors that are high enough then the tolerance limit.

### 6.3.3 Comparison between LQR and LQR Integrator Control Method Performance in Square Trajectory Pattern

The quadrotor flight behavior in tracing the waypoint trajectory in a box pattern is visualized in Fig. 19 (a, b) and their characteristics as shown in Table 14.

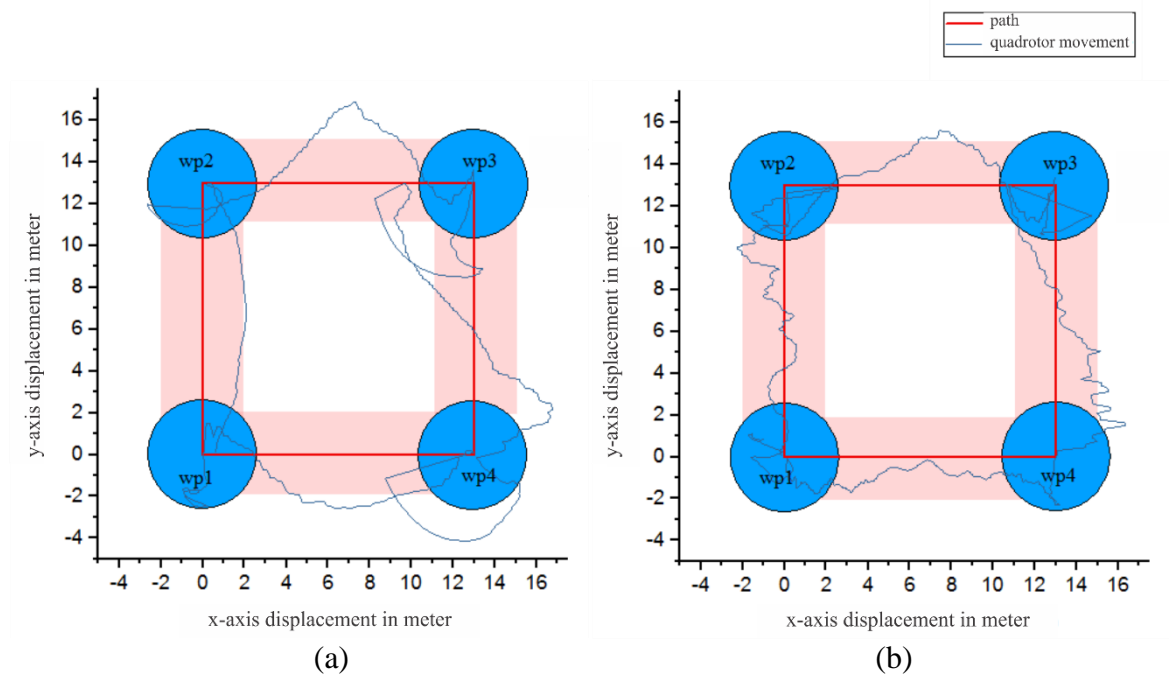


Fig. 19: Quadrotor movement in square trajectory pattern (a) using LQR control (b) using LQR Integrator control.

Based on Table 14, the lack of the LQR control system applied to the quadrotor to trace the waypoint coordinates is corrected by adding an Integrator control to the LQR control. Using LQR and Integrator control, the quadrotor can reduce the steady-state error and multiple overshoots that occur, followed by an increase in the accuracy of tracking aircraft movements on the trajectory from 64.84% to 94.96%. The steady-state error is minimized from 2 meters to 0.54. meters and the average undershoot is -1.04, so there are no multiple overshoots when the quadrotor takes advantage of this control. Based on the

description in the previous paragraph, the Integrator can compensate for the control signal generated by the LQR. The control signal has calculated from an error value multiplied by the last gain integrator. So, the system response does not only depend on giving the current read state value. Besides, this control can accommodate the quadrotor's attitude towards the regulator with the energy required by the system specifications for the 12 steady states.

Table 14: Comparison of Characteristics Movement Quadrotor using LQR and LQR Integrator Control Method in Square Trajectory Pattern

Waypoint	Length of Track (m)	LQR				LQR Integrator			
		Over shoot (m)	Unders hoot (m)	Steady state error (m)	Accu racy (%)	Over shoot (m)	Unders hoot (m)	Steady state error (m)	Accu racy (%)
wp1 to wp2	13	0	0	1.51	86.40	0	0	0.39	93.58
wp2	0	0	-0.15	0	92.22	0	0	0	100
wp2 to wp3	13	0	0	2.10	66.67	0	0	0.45	94.59
wp3	0	0	-2.25	0	20.62	0	0	0	100
wp3 to wp4	13	0	0	2.54	40.29	0	0	0.29	72.73
wp4	0	0	-1.74	0	48.42	0	0	0	100
wp4 to wp1	13	0	0	1.80	65.78	0	0	1.02	98.78
wp1	0	0	-0.01	0	98.34	0	0	0	100
<b>Average</b>		<b>0</b>	<b>-1.04</b>	<b>2.00</b>	<b>64.84</b>	<b>0</b>	<b>0</b>	<b>0.54</b>	<b>94.96</b>

### 6.3.4 Comparison between LQR and LQR Integrator Control Method Performance in Zig – Zag Trajectory Pattern

Comparison of translational motion control is also carried out in zig-zag trajectory tracing, where the quadrotor provides flight characteristics interpreted in Fig. 20 (a, b).

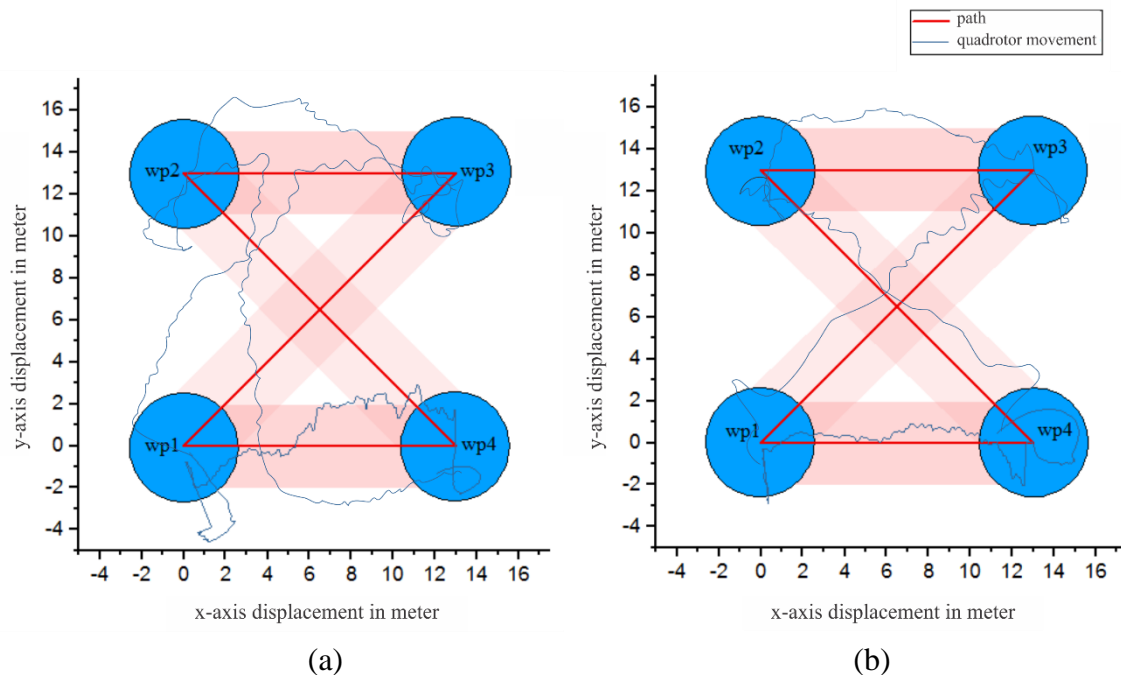


Fig. 20: Quadrotor movement in zig-zag trajectory pattern (a) using LQR method (b) using LQR Integrator method.

Based on Fig. 20 (a, b), the quadrotor has been able to enter within the tolerance of the zig-zag waypoint path when carrying out a search strengthened by the acquisition of data analysis results in Table 15.

Table 15: Comparison of characteristics movement quadrotor using LQR and LQR Integrator control method in Zig – Zag trajectory pattern

Waypoint	Length of Track (m)	LQR				LQR Integrator			
		Over shoot (m)	Unders hoot (m)	Steady state error (m)	Accu racy (%)	Over shoot (m)	Unders hoot (m)	Steady state error (m)	Accu racy (%)
wp1 to wp2	13	0	0	0.76	73.72	0	0	0.18	98.47
wp2	0	0	0	0	100	0	0	0	100
wp2 to wp3	18.38	0	0	4.70	16.15	0	0	0.90	92.36
wp3	0	0	-0.86	0	41.67	0	-0.02	0	93.33
wp3 to wp4	13	0	0	2.24	40.48	0	0	1.84	92.36
wp4	0	0	-0.42	0	84.61	0	-0.1	0	92.85
wp4 to wp1	18.38	0	0	5.08	0	0	0	1.29	95.45
wp1	0	0	-2.45	0	17.24	0	-0.41	0	76
<b>Average</b>		<b>0</b>	<b>-1.12</b>	<b>3.19</b>	<b>46.73</b>	<b>0</b>	<b>-0.18</b>	<b>1.06</b>	<b>86.49</b>

Referring Table 15, it indicates that controlling a quadrotor on a zig-zag line is more complicated than tracing a straight path pattern. This result is evidenced by the more minor accuracy results for the two control method applications. Quadrotor control with LQR control has decreased tracking accuracy to 46.73% with steady-state error, and the average undershoot is getting greater to be 3.19 and -1.12 meters. Likewise, quadrotor control using LQR and Integrator experienced a decrease in tracking accuracy to 86.49% with a steady-state error and an undershoot that occurred at 1.06 and -0.18 meters.

This condition occurs because the zig-zag trajectory pattern requires the quadrotor to rotate by maintaining a direction that exceeds 90°. The results in the yaw torque were significantly affecting the pitch and roll torque being unstable with a greater force. This instability cannot be handled by quadrotor translation control, which has a more extended control update rate than other state controls and makes the quadrotor have a more significant deviation than before. The condition does not necessarily increase the value of gain  $K$ , that resulting torsional the greater torque. The torque can make the quadrotor more responsive rotate in the direction of the x-axis or y-axis even slammed [30]. Therefore, the best system response is presented using the results of the  $Q$  element tuning with a gain  $K$  as in controlling the translation motion at a specific location.

## 7. CONCLUSION

Implementing the LQR control method with the Integrator on the waypoint mission has successfully minimized steady-state error and multiple-overshoot. LQR Integrator can increase the accuracy to 94.96% with a steady-state error of 1.06 meters in square track pattern and 86.49% with a steady-state error of 0.54 meters in zig-zag trajectory. The compensation of Integrator has higher accuracy that can sign to provide minimum error, but it no more effective to increase precision state in translation movement.

In the future, this research needs to develop other methods that can enhance the precision state in quadrotor systems. We will implement an artificial intelligence approach



to combine in anatomy structure LQR control method. So, the system has a self-learning ability that can adapt to the environment dynamically.

## REFERENCES

- [1] Kenzo N, Farid K, Satoshi S, Wei W, Daisuke N. (2010) Autonomous flying robot - unmanned aerial vehicle and micro aerial vehicle. Springer Tokyo Dordrecht Heidelberg London New York. doi: 10.1007/978-4-431-53856-1
- [2] Tri KP, Agfi EP, Andi D. (2015) Optimizing control based on ant colony for quadrotor stabilization. IEEE International Conference on Aerospace Electronics and Remote Sensing Technology, pp 1-4. doi: 10.1109/ICARES.2015.7429820
- [3] Luis RGC, Alejandro EDL, Rojrlío L, Claude P. (2013) Quad rotorcraft control (vision - based hovering and navigation), Springer Verlag London. doi: 10.1007/978-1-4471-4399-4
- [4] Jhon O, Rolf R. (2005) Waypoint guidance for small UAVs in wind, AIAA Virginia University of Washington, 6951: 1-12. <https://doi.org/10.3182/20131120-3-FR-4045.00005>
- [5] Richard S, Mark K, Qi G. (2016) Unscented guidance for waypoint navigation of a fixed-wing UAV, American Control Conference (ACC) Boston, pp 473-478. doi: 10.1109/ACC.2016.7524959
- [6] Anibal O, Bruno S. (2020) Aerial robotic manipulation (research, development and applications), Springer Tracts in Advanced Robotics, 129. doi: 10.1007/978-3-030-12945-3
- [7] When-Ci L, Wun-Shin W. (2016) Design of an automatic docking system for quadcopters, Asia-Pacific Conference on Intelligent Robot, pp 199-203. doi: 10.1109/ACIRS.2016.7556212
- [8] Nurul AI, Nor LO, Dwi P, Z MZ, Luhur B. (2015) Attitude Control of Quadrotor, ARPN Journal of Engineering and Applied Sciences, 10(22): 17206-17211.
- [9] Oktaf AD, Andi D, Tri KP. (2017) Model of linear quadratic regulator (LQR) control method in hovering state of quadrotor. Journal of Telecommunication, Electronic and Computer Engineering, 9(3): 135-143. <https://jtec.utem.edu.my/jtec/article/view/1589/1891>
- [10] Lucas A, Willian CR, Paulo ES, Renato AA. (2013) PID, LQR and LQR-PID on a quadcopter platform. IEEE International Conference on Informatics, Electronics and Vision, pp 1-6. doi: 10.1109/ICIEV.2013.6572698
- [11] Emre CS, Ali TK. (2014) Optimal path tracking control of a quadrotor UAV, IEEE International Conference on Unmanned Aircraft Systems, pp. 115-125. doi: 10.1109/ICUAS.2014.6842246
- [12] Josias GB, Darielson AS, Laurinda LN, Lucas VOF, Kaio MR, Antonio BSJ, Wilkley BC. (2019) Performance comparison between the PID and LQR controllers applied to robotic manipulator joint. IEEE 45<sup>th</sup> Annual Conference of the IEEE Industrial Electronics Society, pp 479-484. doi: 10.1109/IECON.2019.8927059
- [13] Michael FE. (2015) LQR with integral feedback on a parrot mini-drone, MIT Cambridge, 02139.
- [14] Gusna HT, Andi D. (2017) Sistem kendali autopilot pada quadrotor untuk menuju titik koordinat dengan memanfaatkan GPS, Universitas Gadjah Mada, Indonesia.
- [15] Anup V, Pabba S, Jansi KR. (2017) Fully autonomous UAV. IEEE International Conference on Technical Advancements in Computers and Communications, pp 41-44. doi: 10.1109/ICTACC.2017.20
- [16] Lucas VS, Alexandre SB, Mario S-F. (2015) Outdoor waypoint navigation with the AR. Drone quadrotor. IEEE International Conference on Unmanned Aircraft Systems, pp 303-311. doi: 10.1109/ICUAS.2015.7152304
- [17] Tri KP, Andi D, Oktaf AD, Nur ASP. (2016) Optimizing control based on fine-tune PID using ant colony logic for moving control UAV systems. American Institute of Physics Conference Proceedings, 1755, 170011. <https://doi.org/10.1063/1.4958613>
- [18] Mohamad RR, Saeide H, Davoud S. (2013) Designing and simulation for vertical moving control of UAV system using PID, LQR and Fuzzy logic, International Journal of Electrical and Computer Engineering, 3(5):651-659. <http://dx.doi.org/10.11591/ijece.v3i5.3440>



- [19] James WF. (2007) Modelling and linear control of a quadcopter, Cranfield University.
- [20] Katsuhiko O. (2010) Modern control system, 5<sup>th</sup> Edition, Prentice-Hall.
- [21] Russell CH. (2016) Dynamics, 14<sup>th</sup> Edition, Hoboken, New Jersey: Pearson Prentice Hall.
- [22] Zoran B, Petar P, Denis K. (2016) Mathematical modelling of unmanned aerial vehicle with four rotors. *Journal of Interdisciplinary Description of Complex Systems*, 14(1): 88-100. Retrieved from <https://ideas.repec.org/a/zna/indecs/v14y2016i1p88-100.html>
- [23] Gesang N, Andi D. (2017) Undesirable rolling minimization on the EDF missiles flight based on LQR methods, *International Conference on Advanced Mechatronics, Intelligent Manufacture, and Industrial Automation*, pp 85-90. doi:10.1109/ICAMIMIA.2017.8387563
- [24] Andi D, Agfi EP, I MT, Agung W. (2019) The obstacle avoidance system in a fixed-wing UAV when flying low using LQR method. *International Conference on Computer Engineering, Network and Intelligent Multimedia*, pp 1-7. doi: 10.1109/CENIM48368.2019.8973292
- [25] Robert S. (2018) Design and development of the LQR optimal controller for the unmanned aerial vehicle. *Obuda University, Budapest, Hungaria*, 1(36): 45-54. doi:10.19062/1842-9238.2018.16.1.7
- [26] Thomas S, Stefan R. (2017) Eliminating the effect of magnetic disturbances on the inclination estimates of inertial sensors. *IFAC-PapersOnLine*, 50(1): 8798-8803. <https://doi.org/10.1016/j.ifacol.2017.08.1534>
- [27] Karl JA, Tore H. (2006) *Advanced PID control*, ISA Publishing.
- [28] Ariesa BZ, Andi D. (2017) Sistem kendali penghindar rintangan pada quadrotor menggunakan konsep linear quadratic. *Indonesian Journal of Electronics and Instrumentations Systems*, 7(2): 219-230. <https://jurnal.ugm.ac.id/ijeis/article/view/25503/17912>
- [29] Daniele G, Marc SA, Irene A, Maria A, Paolo A, Marco B, Pierluigi DB, Donatella D, Danilo G, Peter Hobbs, Veronika L, Tomasz N, Marco P, Marianna R, Riccardo S, Valerio S, Bernadette S, Fabrizio T. (2020) The use of unmanned aerial vehicles (UAVs) for engineering geology applications, *Springer Bulletin of Engineering Geology and the Environment*, 79: 3437-3481. <https://doi.org/10.1007/s10064-020-01766-2>
- [30] Andi D, Ahmad A, Agfi EP. (2018) Translation movement stability control of quad tiltrotor using LQR and LQG, *International Journal of Intelligent Systems and Applications*, 10(3): 10-21. doi:10.5815/ijisa.2018.03.02